

Exchange effects and large angle proton scattering on light nuclei at intermediate energies: $p + {}^3\text{He}$ scattering

M. S. Abdelmonem

Energy Resources Division, Research Institute, King Fahd University of Petroleum and Minerals, Dhahran, Saudi Arabia

H. S. Sherif

Department of Physics, University of Alberta, Edmonton, Alberta, Canada T6G 2J1

(Received 2 March 1987)

A model developed previously to treat $p + {}^4\text{He}$ scattering at intermediate energies is applied to the case of $p + {}^3\text{He}$ scattering. The scattering amplitude is written as a sum of direct and exchange terms. The direct-plus-knockout exchange terms are approximated by a phenomenological optical potential scattering amplitude. The heavy particle stripping term, representing the exchange of a neutron-proton cluster between projectile and target, is calculated using a modified distorted-wave Born approximation approach. The point-nucleon wave function for the ${}^3\text{He}$ target is determined from a fit to the charge form factor, after subtraction of recently calculated meson exchange current contributions. The back-angle rise in the differential cross section in the energy range 150–600 MeV is reproduced qualitatively when the heavy particle stripping term is included. In addition, a slight improvement in the large angle analyzing power is obtained at 300 and 515 MeV.

I. INTRODUCTION

For many years the behavior of large angle cross sections for proton scattering on light nuclei at intermediate energies has been the subject of several experimental as well as theoretical studies.^{1–5} Complete angular distributions have recently been obtained for $p + {}^4\text{He}$ and $p + {}^3\text{He}$ scattering^{4,5} in the energy range 200–500 MeV and they confirm earlier measurements at higher and lower energies, in that the cross sections at back angles show a rising pattern which is energy dependent. In addition, these recent measurements give almost complete angular distributions for the analyzing powers. It is generally agreed that the behavior of the data at large angles is closely associated with exchange effects involving the projectile and target nucleons. For example, calculations based on the resonating group method, in which the indistinguishability of the nucleons is taken into account have been moderately successful in accounting for data for proton energies up to 150 MeV.⁶ In the intermediate energy range several models have been proposed to treat exchange effects.^{7–12} One of these deals with the treatment of heavy particle stripping (HPS) contribution to the scattering process. The details of the model and its application to $p + {}^4\text{He}$ scattering are given in Ref. 10. The basic ingredient of this approach is the representation of the scattering amplitude as the sum of a phenomenological optical potential amplitude plus a contribution from the HPS mechanism. The latter is calculated using a modified distorted wave Born approximation. The distorted waves used are generated by the same optical potential mentioned above. The potential contains both central and spin-orbit terms and hence one is able to include polarization effects in the discussion. This paper is concerned with the application of the mod-

el to $p + {}^3\text{He}$ scattering. In Sec. II we outline how the HPS amplitude is calculated in this case. The wave function describing the motion of a proton in the ${}^3\text{He}$ target is derived from the ${}^3\text{He}$ charge form factor. The meson exchange current effects calculated by Hadjimichael *et al.*¹³ are subtracted out of the measured charge form factor to enable us to determine a nucleons-only wave function. In Sec. III we present the result of our calculations. Two methods have been used to determine the phenomenological optical potentials: (i) One based on the Schrödinger equation with Woods-Saxon-type complex potentials. (ii) One using the Dirac equation with vector and scalar complex potentials. We compare the two methods and show the differences among the corresponding potentials. The section ends with a discussion of the results and some comments regarding other recent approaches to the present scattering process.

II. CALCULATIONS

The details of the model used here have been given in Ref. 10. The basic idea is to write the elastic scattering amplitude as a sum of direct and exchange terms, then approximate the direct plus knockout exchange terms by an optical potential amplitude. Thus we write

$$T \simeq T_{\text{OM}} - n_p T_{\text{HPS}}, \quad (1)$$

where T_{OM} is the t matrix generated by an optical potential, T_{HPS} is the heavy particle stripping t matrix, and n_p the number of protons in the target (two in the present case).

A modified distorted wave Born approximation is used for T_{HPS} :

$$T_{\text{HPS}} = \langle \phi_{\mu_f}(\mathbf{k}_f, \mathbf{r}_f) \Phi(i, c) | V_{fc} | \Phi(f, c) \chi_{\mu_i}^{(+)}(\mathbf{k}_i, \mathbf{r}_i) \rangle, \quad (2)$$

where $\phi_{\mu_f}(\mathbf{k}_f, \mathbf{r}_f) = e^{i\mathbf{k}_f \cdot \mathbf{r}_f} | \frac{1}{2}\mu_f \rangle$ is a plane wave for the final state p- ^3He relative motion. In the initial state the ^3He target is regarded to be composed of a proton f and a two nucleon cluster c , and is described by the wave function $\Phi(f, c)$. In the final state its wave function is $\Phi(i, c)$. $\chi_{\mu_i}^{(+)}(\mathbf{k}_i, \mathbf{r}_i)$ is an optical potential distorted wave describing the relative motion of the incident proton (with spin projection μ_i) and the ^3He target. The dis-

torted wave is generated by the same optical potential used to calculate T_{OM} .

In Eq. (2), V_{fc} is the interaction potential of proton f with the two nucleons forming cluster c . It is assumed that this potential is spin independent. The target state is assumed to have spin projection ν_i , with the three nucleons in spatial s states. The spin wave function is antisymmetric with respect to the two protons. For the ^3He in the final state we write a similar wave function with spin projection ν_f . After carrying out the spin algebra one gets (we write $\chi_{\mu_i}^{(+)} = \sum_{\mu_i'} \chi_{\mu_i \mu_i'}^{(+)} | \frac{1}{2}\mu_i' \rangle$)

$$T_{\text{HPS}} = \frac{1}{4} \sum_S (2S+1) (S_{\frac{1}{2}}; \nu_f - \mu_i' \mu_i' | \frac{1}{2}\nu_f) (S_{\frac{1}{2}}; \nu_i - \mu_f \mu_f | \frac{1}{2}\nu_i) \\ \times \delta_{\nu_f - \mu_i', \nu_i - \mu_f} \langle e^{i\mathbf{k}_f \cdot \mathbf{r}_f} \Psi(r_{ic}) | V_{fc} | \Psi(r_{fc}) \chi_{\mu_i \mu_i'}^{(+)}(\mathbf{k}_i, \mathbf{r}_i) \rangle, \quad (3)$$

where $S (=0,1)$ is the spin of the n-p cluster in ^3He and Ψ is the s -state spatial wave function of the proton-cluster relative motion. It is assumed that Ψ is independent of S .

The interaction potential V_{fc} is eliminated using the Schrödinger equation satisfied by $\Psi(r_{fc})$. The matrix element in (3) then becomes

$$\langle e^{i\mathbf{k}_f \cdot \mathbf{r}_f} \Psi(r_{ic}) | V_{fc} | \Psi(r_{fc}) \chi_{\mu_i \mu_i'}^{(+)}(\mathbf{k}_i, \mathbf{r}_i) \rangle \\ = \int d\mathbf{r}_i e^{i(\frac{1}{3})\mathbf{k}_f \cdot \mathbf{r}_i} \left[\int d\mathbf{r} e^{-i(\frac{8}{9})\mathbf{k}_f \cdot \mathbf{r}} \Psi(|\mathbf{r}_i + \frac{1}{3}\mathbf{r}|) \left(\frac{\hbar^2}{2m} \nabla^2 - E_b \right) \Psi(\mathbf{r}) \right] \chi_{\mu_i \mu_i'}^{(+)}(\mathbf{k}_i, \mathbf{r}_i), \quad (4)$$

where we have written $\mathbf{r} = \mathbf{r}_{fc}$ and $\mathbf{r}_f = \frac{8}{9}\mathbf{r} - \frac{1}{3}\mathbf{r}_i$. The m is the reduced mass of the proton-cluster system and E_b the relative binding energy. In our numerical calculations, we have assumed the cluster c to have the mass of the deuteron.

The wave function $\Psi(r)$ was derived from a fit to the charge form factor of the ^3He nucleus. In our study¹⁰ of $p + ^4\text{He}$ scattering we found that subtraction of the meson exchange current (MEC) effects from the measured form factors, yielding a nucleons-only wave function, resulted in a noticeable and generally favorable effect on the large angle cross sections. In their recent microscopic study of $p + ^3\text{He}$ scattering, Landau and Sagen¹² find that removal of the MEC effects also affected the large angle scattering. We therefore, use for $\Psi(r)$ a nucleons-only form derived from the form factor after subtracting MEC effects (see note in Ref. 12 concerning the reliability of this procedure). We have used the calculations of Hadjimichael *et al.*¹³ to estimate the MEC contributions to the charge form factor (the difference between the full and the impulse approximation calculations) and subtracted these from the experimental data.¹⁴⁻¹⁷ We then fitted the corrected data using both Eckart-type and the more general sum-of-exponentials wave functions (see Ref. 10). Because of the uncertainties associated with the subtraction procedure mentioned above and with the model dependence of the MEC calculations for large momentum transfer,¹³ we have emphasized the fit to the form factor in the region $q^2 \leq 12 \text{ fm}^{-2}$. The wave function that provided the best fit in this region is the Eckart-type function used earlier by Lim.¹⁸ It has the form

$$\Psi(r) = \frac{N}{r} e^{-\alpha r} (1 - e^{-\beta r})^4, \quad (5)$$

where N is the normalization constant and $\alpha = 0.42 \text{ fm}^{-1}$, $\beta = 1.90 \text{ fm}^{-1}$.

III. RESULTS AND DISCUSSION

In this section we use the t -matrix elements of Eqs. (1) and (3) to calculate the differential cross section and analyzing power for $p + ^3\text{He}$ scattering at the proton incident energies 156, 300, 415, and 515 MeV.²⁸ The data used here are those of Langevin-Juliot *et al.*,¹⁹ Frascaria *et al.*,²⁰ and Hasell *et al.*⁵ We also calculate the cross section at 600 MeV and compare with the data of Fain *et al.*²¹ and Frascaria *et al.*²²

Two methods were used to determine the optical potentials required for the calculations of T_{OM} and the distorted waves used to calculate T_{HPS} . First, the Schrödinger equation code MAGALI,²³ which uses standard Woods-Saxon forms for the potential, was used. The potential consists of a central term plus a spin-orbit term involving the spin of the incident (or outgoing) proton. Other terms dependent on the target spin, such as spin-spin, tensor, or target spin-orbit interactions, could, in principle, be present. The latter will mainly affect the ^3He spin observables, which are not considered here; otherwise, it will add onto the overall central potential that is determined by fitting the data. The effects of the two former interactions on the cross section and the proton analyzing power are found to be small at low energies²⁹ and are expected to be even smaller at intermedi-

ate energies. Only the data forward of a given angle were included in the search (for example, at 300 MeV the cross section data forward of 90° and the A_y data forward of 80° were used). This procedure leads to generally acceptable fits to the data. We refer to these potentials as SWS potentials (Schrödinger-Woods-Saxon).

Because of the recent success of the Dirac phenomenology in reproducing the elastic scattering data at intermediate energies, we also used the Dirac equation computer code RUNT (Ref. 24) to fit the elastic data. As is usual in the Dirac approach, only the projectile nucleon motion is treated "relativistically." The potential comprises scalar and timelike vector terms (similar to the case of nucleons scattered from spin-0 targets). Other terms could be present since we deal with a spin- $\frac{1}{2}$ target, but for simplicity these are not included. Note that we are not after a full relativistic treatment of the $p + {}^3\text{He}$ scattering process, but rather we seek to exploit the ability of the Dirac phenomenology to provide a better fit to the elastic data. Thus our procedure is to obtain, from the Dirac vector and scalar potentials determined by fitting the forward angle data, their Schrödinger equivalent potentials, which we shall refer to here as the Dirac equation-based (DEB) optical potentials.²⁵ These latter potentials, when used in Schrödinger equation calculation, yield the same T_{OM} as that resulting from the Dirac equation code. In Fig. 1 we show the elastic cross section calculation at 300 MeV for scattering angles greater than 60° . The short-dashed curve [labeled OM (SWS)] and the long-dashed curve [labeled OM (DEB)] are nearly equivalent to $\theta \approx 70^\circ$ (the curves coincide forward of 60°). There are large differences between the two curves at extreme backward angles, with the SWS calculation showing a much smaller cross section. In Fig. 2 the results are shown for the analyzing power. Here, again, the SWS and DEB fits are equivalent to $\theta \sim 60^\circ$, but differ beyond this angle. At angles larger than 100° , the SWS potentials give a large negative analyzing power, whereas the DEB calculations show a much smaller A_y . In general, the DEB potentials are found to be in better agreement with the data over the energy range studied here.

The radial shapes of the central parts of these potentials are compared in Fig. 3. We note that the usual feature of the DEB real central potential turning repulsive at short distances, in this energy region, is present. By contrast, the SWS real potential (dashed curve) is repulsive over the entire radial range. The DEB imaginary central potential shows a surface enhancement, indicative of contributions from both volume and surface terms. Its SWS counterpart, however, does not show this feature. It is a purely volume-type potential. The spin-orbit potentials (not shown) have generally the same shape with the DEB potentials about twice as strong as those resulting from the SWS analysis. In Fig. 4 we show the energy dependence of the real central DEB potentials in the energy range 156–600 MeV. The energy dependence is not that much different from what has been observed in heavier nuclei.^{26,27} Note that there is a persistent attractive pocket in the outer region at the higher energies, a feature which characterizes the DEB

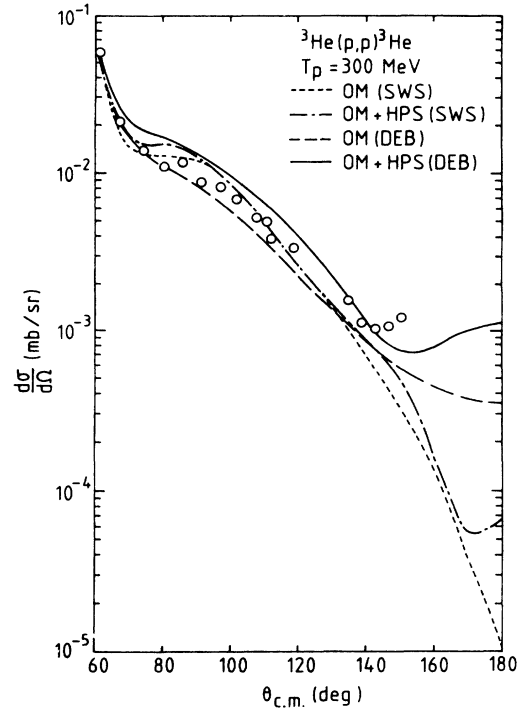


FIG. 1. The large angle differential cross section for $p + {}^3\text{He}$ elastic scattering at $T_p = 300$ MeV. The short-dashed curve [OM (SWS)] represents a fit using the Schrödinger equation with Woods-Saxon optical potentials and the long-dashed curve [OM (DEB)] is the corresponding fit using the Dirac equation-based optical potentials. The dash-dot and solid curves show the effect of including the heavy particle stripping (HPS) contribution to each of the above calculations, respectively. The data are from Ref. 5.

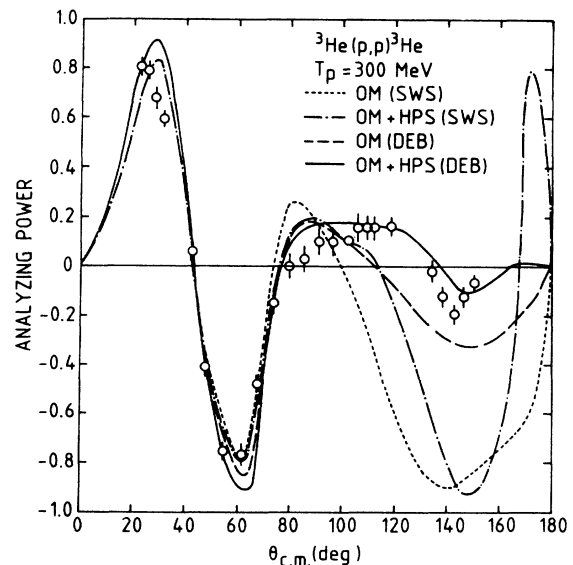


FIG. 2. The analyzing power for $p + {}^3\text{He}$ elastic scattering at $T_p = 300$ MeV. The curves are the same as in Fig. 1. The data are from Ref. 5.

potentials.

We now turn to the HPS contribution. We performed calculations using both the SWS and DEB potentials. The results for the cross section are shown by the dash-dot and solid curves in Fig. 1. We note that when the HPS amplitude is added it causes the cross section to increase sharply at extreme backward angles. This is qualitatively what the large angle data seem to suggest. The calculations with DEB potentials show an increase in the cross section starting at angles near 60° . The effect is less dramatic for the SWS potentials. The latter still give much too low a cross section at back angles.

The analyzing power comparisons are shown in Fig. 2. The solid curve represents the full calculation using the DEB potentials and the dash-dot curve corresponds to the SWS potential. Clearly the final result depends on the potentials. In both cases the inclusion of the HPS changes A_y at large angles. In the present case the com-

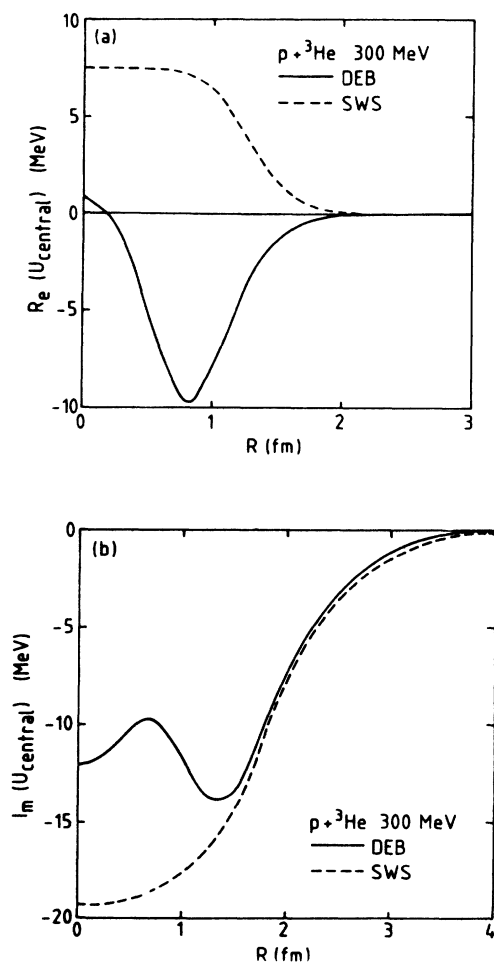


FIG. 3. (a) Real and (b) imaginary parts of the central optical potential for $p + {}^3\text{He}$ scattering at $T_p = 300$ MeV. The dashed curves result from the use of the Schrödinger equation with Woods-Saxon potentials (SWS). The solid curves are the corresponding Dirac equation-based optical potentials (DEB).

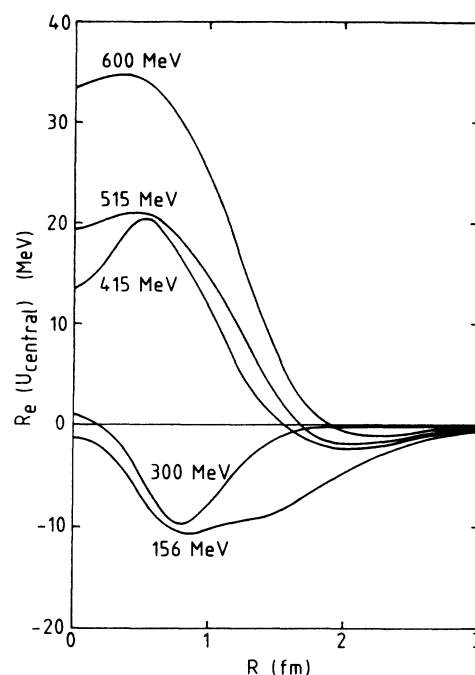


FIG. 4. The energy dependence of the real part of the central DEB optical potential for $p + {}^3\text{He}$ elastic scattering.

ination of DEB + HPS gives results that are reasonably in accord with the data (however, see below for comparisons at other energies). Noting this sensitivity of the HPS calculations to the optical potentials used and in view of the success of Dirac phenomenology (or equivalently the DEB potentials) in describing elastic scattering data both for other nuclei and for the forward angle region in the present case, we shall in the remainder of this discussion use only the DEB potentials.

In Fig. 5 we show the cross section data over the entire angular range for proton energies 156–600 MeV. The calculation with T_{OM} using the DEB potentials are shown as dashed curves. Those that include the HPS contribution are represented by solid curves. We note that in every case the addition of HPS raises the cross section at back angles. The effect is energy dependent and reflects the momentum space behavior of the target wave function. At 156 MeV the effect overestimates the cross section at extreme back angles, whereas at the higher energies the cross section is underestimated. In some instances (e.g., at 515 MeV) the detailed behavior of the data is not reproduced. Again we note here that the addition of HPS, even though it improves the situation somewhat, does not provide detailed agreement with the data at large angles.

The comparisons for the polarization data at 156 MeV and for the analyzing power data at 300, 415, and 515 MeV are shown in Fig. 6. At 156 MeV there are no

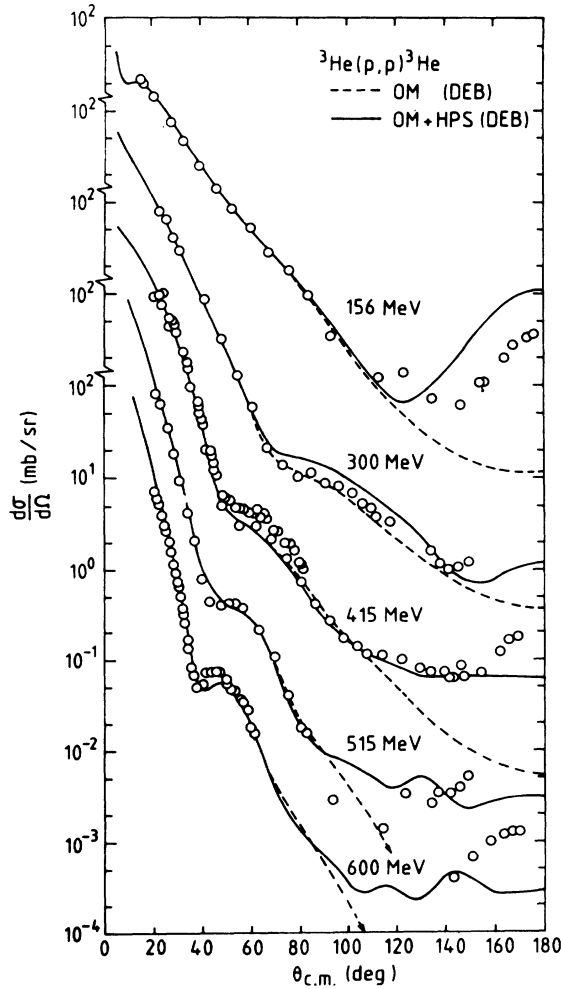


FIG. 5. The differential cross sections for $p + {}^3\text{He}$ elastic scattering for $T_p = 156\text{--}600$ MeV. The data are from Refs. 5 and 19–22. The dashed curves are optical model fits using the DEB potentials. The solid curves include the heavy particle stripping (HPS) contribution.

large angle data. As mentioned earlier, the addition of HPS improves the accord with the data at 300 MeV. At 415 MeV, however, the slight improvement that is gained for angles larger than 120° is clearly at the expense of the agreement with data in the angle range $\theta = 80^\circ\text{--}120^\circ$. At 515 MeV, addition of HPS brings the theoretical calculations somewhat closer to the data for $\theta > 120^\circ$. Again, we see that for the analyzing power there is slight improvement at 300 and 515 MeV, but detailed agreement is lacking.

Two microscopic calculations have been reported recently for the $p + {}^3\text{He}$ system in the energy range considered in the present work. The first¹² is a microscopic first-order momentum space optical potential calculation with antisymmetrized nucleon-nucleon amplitudes. The second is a Glauber model calculation⁵ which includes terms up to triple scattering contributions. Both calcu-

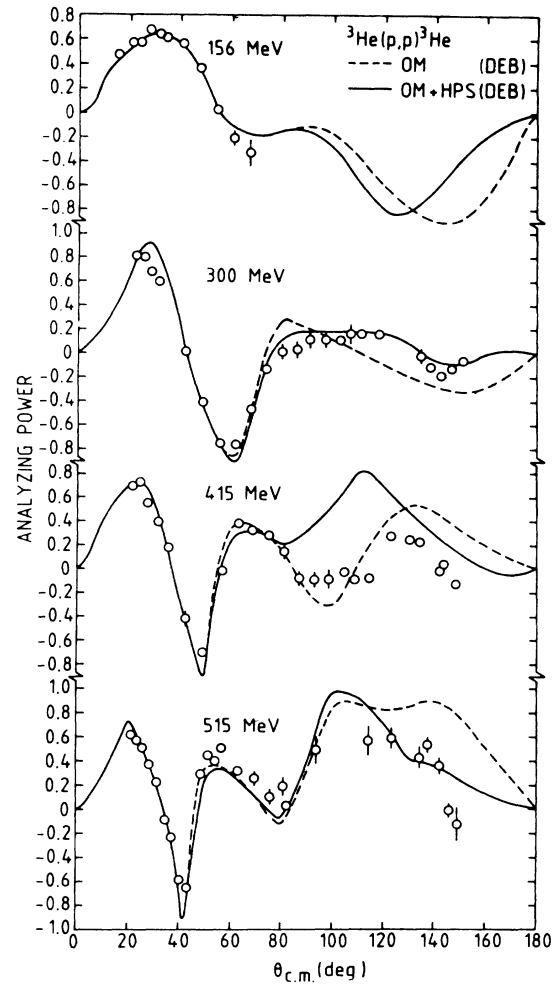


FIG. 6. The polarization data for $p + {}^3\text{He}$ elastic scattering at 156 MeV (Ref. 20) and the analyzing power data at 300, 415, and 515 MeV (Ref. 5). The dashed curves are optical model fits using the DEB potentials. The solid curves include the heavy particle stripping contribution.

lations give good qualitative agreement with the data and are quite encouraging since both are parameter free calculations. The obvious shortcoming of these calculations is their failure to reproduce the analyzing power in the mid-angular range near $60^\circ\text{--}80^\circ$. This indicates that there are some contributions in our phenomenological potentials that are missing in the microscopic calculations. The Glauber calculations show that triple scattering contributions are important at back angles and lead to a flattening of the cross sections in this angular range. The calculations of Ref. 12 also show that the antisymmetrization of the NN amplitudes leads to enhancement of the back angle cross section. Our present calculations show that the heavy particle stripping contributions are also important at these back angles. The lack of detailed agreement with the data, in any of these approaches, emphasizes the fact that none of them encompasses all the

physics of the process. In our particular case the model does not include the contributions from the knockout process for scattering at larger angles. A possible way to remedy this is to replace our phenomenological optical potential by one calculated following a procedure similar to that of Landau and Sagen (preferably with higher order corrections included in the hope of improving the accord with the forward angle data). This then should

be complimented by the calculation of the HPS contribution along the lines outlined in the present work.

ACKNOWLEDGMENTS

The authors are grateful to R. Frascaria and D. Hasell for providing tables of the experimental data. This work was supported in part by the Natural Sciences and Engineering Research Council of Canada.

-
- ¹G. Igo, Nucl. Phys. **A374**, 253c (1982), and references therein.
- ²J. Berger, J. Dufflo, L. Goldzahl, F. Plouin, J. Oostens, M. vanden Dossche, L. Vu Hai, G. Bizard, C. LeBrun, F. L. Fabbri, P. Picozza, and L. Satta, Phys. Lett. **63B**, 111 (1976); Phys. Rev. Lett. **37**, 1195 (1976).
- ³P. Berthet, R. Frascaria, B. Tatischeff, J. Banaigs, J. Berger, J. Dufflo, L. Goldzahl, F. Plouin, M. Boivin, F. Fabbri, P. Picozza, and L. Satta, Phys. Lett. **106B**, 465 (1981).
- ⁴G. A. Moss, L. G. Greeniaus, J. M. Cameron, D. A. Hutcheon, R. L. Liljestrang, C. A. Miller, G. Roy, B. K. S. Koene, W. T. H. van Oers, A. W. Stetz, A. Willis, and N. Willis, Phys. Rev. C **21**, 1932 (1980).
- ⁵D. K. Hasell, A. Bracco, H. P. Gubler, W. P. Lee, W. T. H. van Oers, R. Abegg, D. A. Hutcheon, C. A. Miller, J. M. Cameron, L. G. Greeniaus, G. A. Moss, M. B. Epstein, and D. J. Margaziotis, Phys. Rev. C **34**, 236 (1986).
- ⁶I. Reichstein, D. R. Thompson, and Y. C. Tang, Phys. Rev. C **3**, 2139 (1971); P. Heiss and H. H. Hackenbroich, Nucl. Phys. **A182**, 522 (1972); D. R. Thompson, R. E. Brown, M. Lemere, and Y. C. Tang, Phys. Rev. C **16**, 1 (1977); P. N. Shen, Y. C. Tang, H. Kanada, and T. Kaneko, *ibid.* **33**, 1214 (1986).
- ⁷B. Z. Kopeliovich and I. K. Potashnikova, Yad. Fiz. **13**, 1032 (1971) [Sov. J. Nucl. Phys. **13**, 592 (1971)].
- ⁸H. Lésniak, L. Lésniak, and A. Tekou, Nucl. Phys. **A267**, 503 (1976).
- ⁹H. S. Sherif and R. S. Sloboda, Phys. Lett. **99B**, 369 (1981).
- ¹⁰H. S. Sherif, M. S. Abdelmonem, and R. S. Sloboda, Phys. Rev. C **27**, 2759 (1983).
- ¹¹M. J. Paez and R. H. Landau, Phys. Rev. C **29**, 2267 (1984); Phys. Lett. **142B**, 235 (1985).
- ¹²R. H. Landau and M. Sagen, Phys. Rev. C **33**, 447 (1986).
- ¹³E. Hadjimichael, B. Goulard, and R. Bornais, Phys. Rev. C **27**, 831 (1983).
- ¹⁴H. Collard, R. Hofstadter, E. B. Hughes, A. Johansson, M. R. Yearian, R. B. Day and T. R. Wagner, Phys. Rev. **138**, B57 (1965).
- ¹⁵J. S. McCarthy, I. Sick, R. R. Whitney, and M. R. Yearian, Phys. Rev. Lett. **25**, 884 (1970).
- ¹⁶J. S. McCarthy, I. Sick, and R. R. Whitney, Phys. Rev. C **15**, 1396 (1977).
- ¹⁷R. G. Arnold, B. T. Chertok, S. Rock, W. P. Schütz, Z. M. Szalata, D. Day, J. S. McCarthy, F. Martin, B. A. Mecking, I. Sick, and G. Tamas, Phys. Rev. Lett. **40**, 1429 (1978).
- ¹⁸T. K. Lim, Phys. Lett. **43B**, 349 (1973).
- ¹⁹H. Langevin-Joliot, Ph. Narboni, J. P. Didelez, G. Duhamel, L. Marcus, and M. Roy-Stephan, Nucl. Phys. **A158**, 309 (1970).
- ²⁰R. Frascaria, Ph. Narboni, V. Comparat, N. Marty, M. Morlet, and A. Willis, Lett. Nuovo Cimento **2**, 240 (1971).
- ²¹J. Fain, J. Gardes, A. Lefort, L. Meritet, J. F. Pauty, G. Peynet, M. Querrou, F. Vazeille, and B. Ille, Nucl. Phys. **A262**, 413 (1976).
- ²²R. Frascaria, I. Brissaud, N. Marty, M. Morlet, F. Reide, A. Willis, R. Beurtey, A. Boudard, M. Garcon, G. A. Moss, Y. Terrien, and W. T. H. van Oers, Phys. Lett. **66B**, 329 (1977).
- ²³J. Raynal, private communication.
- ²⁴E. D. Cooper, Ph.D. thesis, University of Alberta, 1981 (unpublished), and private communication.
- ²⁵H. S. Sherif, R. I. Sawafta, and E. D. Cooper, Nucl. Phys. **A449**, 709 (1986).
- ²⁶M. Jaminon, C. Mahaux, and P. Rochus, Phys. Rev. C **22**, 2027 (1980).
- ²⁷B. C. Clark, S. Hama, and R. L. Mercer, in *The Interaction Between Medium Energy Nucleons in Nuclei*, AIP Conf. Proc. No. 97 edited by H. Meyer, (AIP, New York, 1982), p. 260.
- ²⁸The data at 200 MeV (Ref. 5) extend only to $\theta_{c.m.} = 121^\circ$ and are reasonably fitted using T_{OM} alone. The effects of T_{HPS} appear at angles larger than 120° at this energy and hence these data do not test the HPS contributions. For this reason they have been excluded from the present analysis.
- ²⁹H. S. Sherif, Phys. Rev. C **19**, 1649 (1979).